Osmotrophy of dissolved organic carbon by coccolithophores in darkness

Jelena Godrijan[1,2] (ID), **David T. Drapeau**[1] (ID) and **William M. Balch**[1] (ID)

[1]Bigelow Laboratory for Ocean Sciences, East Boothbay, ME 04544, USA; [2]Division for Marine and Environmental Research, Ruđer Bošković Institute, Zagreb 10000, Croatia

Author for correspondence:
Jelena Godrijan
Email: jelena.godrijan@irb.hr

Summary

- The evolutionary and ecological story of coccolithophores poses questions about their heterotrophy, surviving darkness after the end-Cretaceous asteroid impact as well as survival in the deep ocean twilight zone. Uptake of dissolved organic carbon might be an alternative nutritional strategy for supply of energy and carbon molecules.
- Using long-term batch culture experiments, we examined coccolithophore growth and maintenance on organic compounds in darkness. Radiolabelled experiments were performed to study the uptake kinetics. Pulse–chase experiments were used to examine the uptake into unassimilated, exchangeable pools vs assimilated, nonexchangeable pools.
- We found that coccolithophores were able to survive and maintain their metabolism for up to 30 d in darkness, accomplishing about one cell division. The concentration dependence for uptake was similar to the concentration dependence for growth in *Cruciplacolithus neohelis*, suggesting that it was taking up carbon compounds and immediately incorporating them into biomass. We recorded net incorporation of radioactivity into the particulate inorganic fraction.
- We conclude that osmotrophy provides nutritional flexibility and supports long-term survival in light intensities well below threshold for photosynthesis. The incorporation of dissolved organic matter into particulate inorganic carbon, raises fundamental questions about the role of the alkalinity pump and the alkalinity balance in the sea.

Introduction

Coccolithophores are unicellular, photosynthetic algae of the eukaryotic class Haptophyta (Adl *et al.*, 2019) that are covered in calcium carbonate scales, coccoliths (Taylor & Brownlee, 2016) and are one of the major drivers of the ocean's carbon cycle (Winter & Siesser, 1994; Langer, *et al.*, 2021). Coccolithophores influence the carbon cycle by means of two fundamental 'pumps': (1) the biological pump, in which those heavy coccoliths increase the sinking rate of particulate organic carbon (POC), with subsequent faster rates of CO_2 drawdown (Rost & Riebesell, 2004); and (2) the alkalinity pump, in which they decrease alkalinity through the calcification process producing both CO_2 and particulate inorganic carbon (PIC), in the form of calcified coccoliths. Therefore, the net effect of coccolithophores on the carbon cycle depends on the balance of their CO_2 raising by an alkalinity pump and their CO_2 lowering by facilitating the organic biological pump. Moreover, it is assumed that the PIC found in coccoliths originates from dissolved inorganic carbon (DIC), not dissolved organic carbon (DOC) (Paasche, 2001; Brownlee & Taylor, 2004; Bach *et al.*, 2013).

Coccoliths accumulate on the ocean floor forming deep-sea sediments and represent a major constituent of the calcareous nannofossil record (Bown, 1998). These records reveal that this

algal group evolved in late Triassic period (*c.* 225 million years ago (Ma)) and by the Cretaceous period it was a major component in the open ocean algal assemblages (Bown *et al.*, 2004). At the Cretaceous–Paleogene (K/Pg) boundary, 66 Ma, an asteroid impact caused a mass extinction event on Earth, with a loss of > 90% of coccolithophore species (Bown *et al.*, 2004). Far less catastrophic extinction rates have been inferred from fossils of coastal primary producers such as diatoms and dinoflagellates, probably due to their greater trophic flexibility and their ability to form resting cysts (Ribeiro *et al.*, 2011). There are no reports of resting cysts for coccolithophores, possibly with the exception of *Braarudosphaera*, which is not a typical coccolithophore because it is extracellularly calcified and morphologically similar in shape and texture to resting cysts (Jones *et al.*, 2021). Together with the associated ocean acidification and cooling, the impact caused the suppressed light intensities responsible for a massive drop in primary production (Vajda *et al.*, 2015; Gibbs *et al.*, 2020). Nonetheless, coccolithophores survived and recovered as one of the dominant phytoplankton groups in the modern ocean. Today they are inhabiting both the coastal and oceanic realms (Godrijan *et al.*, 2018; Balch *et al.*, 2019; de Vries *et al.*, 2021), with some species even thriving in subeuphotic environments, at light intensities well below those required to support photosynthesis (Poulton *et al.*, 2017; Balch *et al.*, 2019).

A possible strategy for the survival of coccolithophores in a low-light environment is mixotrophy and acquiring carbon from a diverse set of organic carbon sources. Mixotrophy is a nutritional strategy in which autotrophy and heterotrophy are combined within a single organism (Worden *et al.*, 2015). Recently a new term has been coined, mixoplankton, covering mixotrophic plankton that combine phototrophy and phagotrophy (Flynn *et al.*, 2019). Haptophytes, including coccolithophores, have been shown to have the ability to phagocytise particles (phagotrophy) (Parke *et al.*, 1956; Parke & Adams, 1960; Houdan *et al.*, 2006; Avrahami & Frada, 2020). Osmotrophs, conversely, absorb DOC that they use for their nutrition and/or carbon sources. Far less is known about the ability of coccolithophores to take up and assimilate DOC (Blankley, 1971; Godrijan *et al.*, 2020). Here we report evidence of coccolithophore osmotrophy through long-term survival in darkness as well as the kinetics of organic carbon uptake and its assimilation into POC.

Specifically, we focus on the uptake of three organic compounds: acetate, mannitol and glycerol, selected on the basis of our screenings in a previous work of a large array of organic compounds as possible carbon sources for coccolithophores (Godrijan *et al.*, 2020). Acetate, an organic salt with two carbon atoms, is common in marine ecosystems and is an important carbon and energy source for microbes (Wu *et al.*, 1997; Zhuang *et al.*, 2019). Use of acetate as a carbon source in microalgae cultivation is concentration dependent, lower concentrations have been found to stimulate growth (Qiao & Wang, 2009), while higher concentrations have been shown to be inhibiting or even toxic (Wood *et al.*, 1999; Jeon *et al.*, 2006). Mannitol, a sugar alcohol with six carbon molecules, has been found to be taken up by some microalgae and has growth stimulating effects (Colman *et al.*, 1986; Yee, 2015). Glycerol is a polyol compound with three carbon atoms. Multiple strains of algae are able to take up and grow rapidly on glycerol (Wood *et al.*, 1999; O'Grady & Morgan, 2011; Perez-Garcia *et al.*, 2011). Some of these studies have been made on economically important microalgae, that is *Chlorella*, *Dunaliella*, *Nannochloropsis* and *Scenedesmus* (Perez-Garcia *et al.*, 2011; Yee, 2015; Silva *et al.*, 2016), while studies on coccolithophores remain sparse to this day (Blankley, 1971).

This paper is fundamentally directed at documenting and quantifying coccolithophore osmotrophy as well as discussing its relevance to their evolutionary history, growth and ecology. We investigated the survival of coccolithophores in darkness by performing growth experiments on different concentrations of the above-mentioned DOC. We also used radiolabel-uptake experiments to estimate cellular kinetic response at environmentally realistic concentrations, and measured the fraction of radiolabelled carbon actually fixed into organic tissue. We tested three hypotheses: (1) coccolithophore cells can grow in darkness on organic compounds; (2) uptake displays Michaelis–Menten kinetics and indicates active transport; and (3) DOC taken up by coccolithophores are assimilated into nonexchangeable pools over time scales of 24 h. The alternative hypothesis was that the uptake of those compounds is associated with passive diffusion across the cell membrane and the material is freely exchangeable even after periods of 24 h. We note that passive transport is

energetically downhill and depends on the chemical or electrochemical gradient (Reuss & Altenberg, 2013). It can sometimes exhibit Michaelis–Menten kinetics, which is more likely to occur for electroneutral mannitol and glycerol than for negatively charged acetate (Nelson, 2002). The findings of this paper address the knowledge gap of osmotrophy in coccolithophores, as well as its evolutionary and ecological significance.

Materials and Methods

Culture strains and growth conditions

We used coccolithophores obtained from the National Center for Marine Algae and Microbiota (NCMA, former Culture Collection of Marine Phytoplankton CCMP). We worked with the strain CCMP289 for the species *Cruciplacolithus neohelis* (McIntyre & Bé) Reinhardt and strain CCMP3337 of *Chrysotila carterae* (Braarud & Fagerland) Andersen, Kim, Tittley & Yoon (NCMA lists the strain as *Pleurochrysis carterae*). These strains were selected based on our previous work on 25 strains of 12 different coccolithophore species, in which we investigated organic matter as possible carbon sources for coccolithophores (Godrijan *et al.*, 2020). We kept the cultures at 22°C (CCMP289) or 16°C (CCMP3337) in L1 enriched seawater medium (Guillard & Hargraves, 1993) at an irradiance of 400 µmol photons $m^{-2} s^{-1}$ from fluorescent lights on a 14 h : 10 h, light : dark cycle. To avoid introducing naturally occurring organic compounds all culture media were based on artificial seawater (Keller *et al.*, 1987). As part of the experimental setup, we subjected the strains to axenic screening by microscopic examination and grew them in a general-purpose test medium to detect the presence of bacteria and fungi in marine cultures (Hallegraeff *et al.*, 2003).

Batch growth experiments

We performed these experiments to determine whether coccolithophores (CCMP289 and CCMP3337) can sustain themselves in darkness by using organic compounds as energy and/or carbon sources.

First, we prepared 350 ml of L1 medium and log phase cells from each strain. The cell concentrations of CCMP289 and CCMP3337 were 5×10^4 cells l^{-1} and 1×10^4 cells l^{-1}, respectively. We then poured 15 ml aliquots into 20 vials. To see how the addition of organics would affect cell growth in the light, we set up four vials under light conditions (Supporting Information Fig. S1a): one vial was a control with no organics added and three separate vials with acetate, mannitol or glycerol at a final concentration of 100 µmol l^{-1} as an intermediate concentration in the range of dark treatments (see later). The remaining 16 vials were kept in darkness (Fig. S1a). Our goal was to determine the effect of concentration on growth: one vial was the control with no organics added and five vials with each organic compound in final concentrations of 10, 30, 100, 300 and 1000 µmol l^{-1}. The experiment lasted for *c.* 30 d; temperature and irradiance for the illuminated cultures were the same as for culture growth and maintenance, vials kept in darkness were also kept at the original

growth temperature and additionally covered in black aluminium foil, to ensure complete darkness. We sampled the vials for cell counts every 2–3 d and during sampling we kept light intensities corresponding to experimental conditions. This time-course experiment was performed without replicates, however we took repeated duplicate samples for cell counts (technical duplicates). Cell concentration was determined using a haemocytometer on an American Optical Microscope (Spencer Lens Co., Buffalo, NY, USA) with polarisation optics for CCMP289, as well as a Moxi Z Cell Counter (Andwin Scientific, Simi Valley, CA, USA) for CCMP3337. The Moxi Z instrument uses Gaussian curve fitting with a coincidence correction algorithm of cell count (vs diameter) histograms to extract precise (> 95%) cell count metrics in a sample. The extracted raw data were further used for cellular carbon calculations of CCMP3337. After the experiment, the vials, which were kept in the dark, were placed in the light, and after 10 d we were able to qualitatively confirm, under the microscope, renewed growth of coccolithophore cells.

Radiolabelled DOC kinetic experiments

To understand the mechanism of DOC compound uptake and to see whether species take up different DOC compounds passively or actively, we performed time-course experiments using $[^{14}C]$-labelled DOC compounds. Specific activities of the radiotracers were 1.9×10^6 µBq µmol^{-1} for $[^{14}C]$acetate, 2.1×10^6 µBq µmol^{-1} for $[^{14}C]$mannitol and 5.9×10^6 µBq µmol^{-1} for $[^{14}C]$glycerol, (PerkinElmer, Waltham, MA, USA).

We prepared a solution of L1 medium and exponentially growing culture of each strain, with final concentrations of 5×10^4 cells l^{-1} and left them at their growth temperature in darkness for 24 h to adapt. We divided the prepared solution in 45 ml aliquots to 24 vials for each compound and strain (Fig. S1b). To quadruplicate vials, we added 0.45 ml of unlabelled DOC compound from six stock solutions (1×10^{-6}, 1×10^{-5}, 1×10^{-4}, 1×10^{-3}, 1×10^{-2} and 1×10^{-1} mol l^{-1}). The experiment started when we then added 0.02 ml of $[^{14}C]$-labelled DOC compound (2 µCi of added radioactivity) to each of 24 vials, giving us final concentrations of organic compounds as stated in Table S1. To one vial from those six concentration-quadruplicates we immediately added 1 ml of buffered formaldehyde to act as a killed control. We then incubated the 18 triplicates and six control vials at their growth temperature in darkness for up to 24 h (Fig. S1b), with the sample timing to examine for linear uptake rates at 15 min, 1, 3 and 24 h. At each sampling, 5 ml of experimental culture were filtered onto a 0.4 µm pore-size, 25 mm diameter polycarbonate filter. We also filtered samples at 24 h for $[^{14}C]$-microdiffusion analysis, which separates the POC fraction from the PIC fraction (Paasche & Brubak, 1994; Balch *et al.*, 2000). Following the microdiffusion step to separate acid-labile (PIC) vs acid-stabile (POC) fractions, each filter was then placed on the bottom of a clean scintillation vial and scintillation cocktail was added (Balch *et al.*, 2000). The radioactivity was measured using a Tri-Carb 3110TR liquid scintillation analyser (PerkinElmer). We calculated the net uptake velocity of $[^{14}C]$-labelled organic compounds using the equations of Parsons *et al.*

(1984) $v = (R_n - R_f) \times W/R \times T$ where v (mol l^{-1} h^{-1}) is the net uptake rate, R_n [Bq] is the sample count, R_f [Bq] is the formalin-killed control count and W (mol l^{-1}) is the total concentration of the organic compound in the sample. R [Bq] is the total activity of the added compound to a sample and T [h] is the number of hours of incubation.

Pulse–chase experiments

To test if the compounds that were taken up were assimilated within the cell, we performed pulse–chase experiments. This method first takes into account the cellular uptake of radiolabelled compound ('pulse') that is then exposed to the same unlabelled compound ('cold chase'), at concentrations far above the labelled one. As an indicator of assimilation, the $[^{14}C]$-labelled DOC compound would not be exchanged when 'chased' with vastly higher concentrations of the same unlabelled compound. Unassimilated compounds in intracellular pools, conversely, would be released from the cell as a new equilibrium between the intracellular and extracellular DOC concentrations is established (Balch, 1986). Following the radiolabelled DOC kinetic experiments, after 24 h, we added the cold chase as 1 ml of 1 M of unlabelled compound to the remaining 25 ml in vials used in the kinetics experiments (Fig. S1c). The addition of 1 ml of an organic compound could induce a substantial osmotic shock that could lead to short-term osmotic shrinkage of the protoplast, before the entry of the organic substance raised the internal osmolarity to the external osmolarity. We therefore measured particulate cellular radioactivity using the procedure described above at 5 min, 20 min and 3 h post chase, which provided three different time scales to evaluate how exchangeable were the intracellular compounds.

## Statistics, data handling and visualisation

To test the effects of added organics on cell counts during growth experiments, we used a one-way ANOVA and Tukey's test for *post hoc* pairwise comparisons. The effects of light and darkness were analysed separately. For the light treatments, we tested the hypothesis that the addition of organics had an effect on cell growth by comparing cell counts during the 30-d experiment of the unamended control with those of three added organics. For the treatments in the dark, we tested the hypothesis that higher concentrations would have a greater effect and analysed each compound separately using cell counts during the 30-d incubation at each concentration treatment. Furthermore, we calculated the carbon content of the cells of CCMP3337 according to the equations for cellular elemental content, based on nine isolates covering a wide range of coccolithophore cell diameters and representative of the taxonomic diversity of coccolithophores (Villiot *et al.*, 2021). The basis for these calculations were cell diameters measured using a Cell Counter Moxi Z instrument, these were averaged from raw data for each sample that was measured and standard deviation of a frequency distribution was calculated. We also calculated the growth rates (µ) by fitting the two-parameter exponential function $y = a\,e^{b\,x}$ to the exponential growth phase

and using the calculated slope (b) as the growth rate. Doubling time (dt) was calculated following the equation: dt = $\log_{e(2)}/\mu$. Growth and uptake experiments were tested against a nonlinear curve fit Michaelis–Menten model $y = V_{max} \times x/(K_m + x)$, with the Levenberg–Marquardt iteration algorithm. For both growth and saturation uptake curves, the kinetic properties, K_m (the affinity with which the cells were taking up the organics, aka half-saturation coefficient) and V_{max} (the maximum rate of growth or uptake) were determined (Haldane, 1957). All statistical analyses were performed using Origin software (OriginLab, Northampton, MA, USA). Graphical representations of data were constructed with ORIGIN and GRAPHER software (Golden software, Golden, CO, USA). Experimental schemes were drawn using symbols courtesy of the Integration and Application Network, University of Maryland Center for Environmental Science (https://ian.umces.edu/symbols/).

Results

Growth

After 30 d in light conditions, *C. neohelis* (CCMP298) reached an average cell count of 4.3×10^6 cells l^{-1}, SD = $\pm 3.7 \times 10^5$ cells l^{-1} in four treatments (control and the three organic compounds), while *C. carterae* (CCMP3337) reached 1.4×10^6 cells l^{-1}, SD = $\pm 2.6 \times 10^5$ cells l^{-1} (Fig. 1). Using all cell counts recorded during the 30-d experiment for each of the light treatments we found no statistically significant differences between the control and the organic compounds, as determined using one-way ANOVA for *C. neohelis* $F_{(3,91)} = 0.142$, $P = 0.935$ and for *C. carterae* $F_{(3,75)} = 0.958$, $P = 0.417$. After a brief lag phase, exponential growth lasted until day 17 for *C. neohelis* and day 21 for *C. carterae* (Table 1). Because there was no statistically significant difference between the light treatments, we averaged the
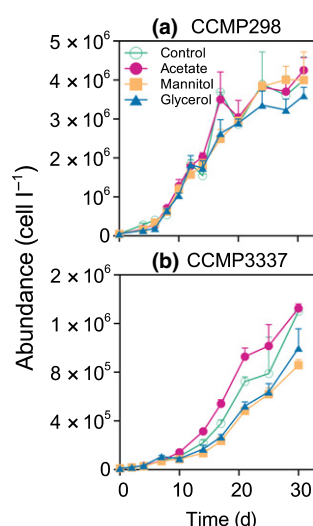
Fig. 1 Cell abundances of CCMP298 *Cruciplacolithus neohelis* (a) and CCMP3337 *Chrysotila carterae* (b) during the 30-d time course in the light with the addition of acetate, mannitol or glycerol at a concentration of 100 μmol l^{-1}. Open circles on the green line represent control without organic compounds. Error bars indicate technical duplicates for cell counts.

cellular growth rates during the exponential phase and they were 0.264 d^{-1} (SD = ± 0.025 d^{-1}) for *C. neohelis* and 0.168 d^{-1} (SD = ± 0.026 d^{-1}) for *C. carterae* (Table 1). Accordingly, *C. neohelis* doubled on average every 2.64 d (SD = ± 0.2 d), whereas *C. carterae* divided every 4.2 d (SD = ± 0.6 d) (Table 1).

Coccolithophores were able to survive for 30 d in darkness (Fig. 2). They were able to accomplish about one division in these conditions. The cell concentrations of *C. neohelis* in dark conditions went from inoculated 5×10^4 cells l^{-1} to maximal 1.1×10^5 cells l^{-1} in 1000 μmol l^{-1} acetate and for *C. carterae* from inoculated 1×10^4 cells l^{-1} to maximal 2.7×10^4 cells l^{-1} in 100 μmol l^{-1} acetate. For *C. neohelis* there was a statistically significant difference in cell counts during the 30-d experiment between applied concentrations (0, 10, 30, 100, 300 and 1000 μmol l^{-1}) in all organic compound treatments as demonstrated by one-way ANOVA. For acetate ($F_{(5,131)} = 12.595$, $P = 5.421 \times 10^{-10}$) a Tukey's *post hoc* test showed that the difference was dose dependent and that the 100, 300 and 1000 μmol l^{-1} concentrations were statistically significantly different compared with the 0, 10, 30 μmol l^{-1} at the $P < 0.05$ level (Fig. S2a). In mannitol ($F_{(5,132)} = 7.039$, $P = 7.320 \times 10^{-6}$) Tukey's *post hoc* test showed significant difference between the two highest concentrations (300 and 1000 μmol l^{-1}) and the two lowest (0 and 10 μmol l^{-1}) at the $P < 0.05$ level (Fig. S2b). In glycerol ($F_{(5,132)} = 17.224$, $P = 4.277 \times 10^{-13}$) Tukey's *post hoc* test showed significant difference between the two highest concentrations (300 and 1000 μmol l^{-1}) and all others at the $P < 0.05$ level (Fig. S2c). For *C. carterae*, there was no statistically significant difference in cell counts during the 30-d experiment between applied concentrations (0, 10, 30, 100, 300 and 1000 μmol l^{-1}) across all compounds (Fig. 3). This was demonstrated using one-way ANOVA for acetate ($F_{(5,108)} = 1.106$, $P = 0.361$), mannitol ($F_{(5,111)} = 1.041$, $P = 0.397$) and glycerol ($F_{(5,108)} = 1.361$, $P = 0.245$).

Between all treatments in the dark, *C. neohelis* cells exhibited the highest growth rates at organic compound concentrations of 1000 μmol l^{-1} 0.027 d^{-1} (SD = ± 0.003 d^{-1}) (Table 1). By contrast, *C. carterae* did not exhibit dose dependence and had low growth rates in all treatments, including the control, averaging 0.018 d^{-1} (SD = ± 0.002 d^{-1}) (Table 1). Furthermore, the potential cell doubling time for *C. neohelis* cells averaged 25.8 d (SD = ± 2.7 d) at a concentration of 1000 μmol l^{-1} when considering all organic compounds. For *C. carterae* (Table 1), average doubling time across all treatments was 39.7 d (SD = ± 3.4 d), while our experiment lasted 30 d. For *C. neohelis*, the calculated K_m for growth was in the range of 10^{-5} mol l^{-1} for all compounds (Fig. 3), while the highest calculated V_{max} was 0.025 d^{-1} (SD = ± 0.003) for acetate. We were unable to perform these calculations for *C. carterae* because the Michaelis–Menten model fit failed (Table S2).

We also followed cell size of *C. carterae* during batch growth experiments. Both cell size and calculated carbon content decreased under light as well as under dark conditions (Table 2), but the decrease was more pronounced under dark conditions across all experimental treatments. During the 30-d period, cell diameter decreased from 9.6 μm to an average of 8.1 μm (SD = ± 0.2 μm) taking into account all light

Table 1 Growth rate (μ) was calculated by fitting the two-parameter exponential function $y = a\,e^{bx}$ to the exponential growth phase and using the calculated slope (b) as the growth rate for period (P) for CCMP298 *Cruciplacolithus neohelis* and CCMP3337 *Chrysotila carterae* in light and dark conditions in each concentration (Conc) of dissolved organic compounds (DOC).

DOC	Conc (μmol l⁻¹)	*C. neohelis* (CCMP298)						*C. carterae* (CCMP3337)					
		μ (d⁻¹)	dt (d)	SE	CI	Prob > F	P (d)	μ (d⁻¹)	dt (d)	SE	CI	Prob > F	P (d)
Light													
Control	0	0.261	2.65	0.021	0.058	4.02×10^{-5}	1–14	0.182	3.80	0.007	0.017	1.64×10^{-7}	1–17
Acetate	100	0.254	2.73	0.027	0.075	1.19×10^{-4}	1–17	0.197	3.51	0.007	0.017	9.33×10^{-8}	1–17
Mannitol	100	0.240	2.89	0.027	0.076	1.50×10^{-4}	1–17	0.151	4.60	0.012	0.032	9.28×10^{-6}	1–17
Glycerol	100	0.299	2.32	0.023	0.064	3.55×10^{-5}	1–17	0.141	4.90	0.019	0.048	9.28×10^{-5}	1–17
Dark													
Control	0	0.009	73.27	0.004	0.010	4.96×10^{-6}	1–20	0.018	38.00	0.004	0.009	1.93×10^{-7}	1–30
Acetate	10	0.008	82.81	0.004	0.012	9.93×10^{-6}	1–24	0.019	35.95	0.003	0.007	2.53×10^{-7}	1–30
	30	0.010	70.59	0.003	0.008	1.69×10^{-9}	1–24	0.018	37.49	0.003	0.008	2.86×10^{-8}	1–30
	100	0.017	39.74	0.002	0.005	1.46×10^{-9}	1–20	0.018	38.51	0.004	0.010	1.03×10^{-6}	1–30
	300	0.022	31.75	0.004	0.009	6.13×10^{-8}	1–20	0.016	43.73	0.004	0.011	2.40×10^{-6}	1–30
	1000	0.024	28.91	0.002	0.004	1.67×10^{-10}	1–24	0.017	41.33	0.004	0.008	1.98×10^{-7}	1–30
Mannitol	10	0.009	79.58	0.003	0.007	1.34×10^{-5}	1–20	0.017	41.58	0.004	0.009	6.30×10^{-8}	1–30
	30	0.013	51.92	0.003	0.009	7.37×10^{-4}	1–20	0.017	42.01	0.003	0.007	7.99×10^{-9}	1–30
	100	0.021	32.44	0.004	0.011	6.11×10^{-7}	1–17	0.021	32.74	0.003	0.007	1.64×10^{-8}	1–30
	300	0.026	26.38	0.006	0.017	2.75×10^{-5}	1–17	0.017	41.09	0.003	0.007	4.81×10^{-8}	1–30
	1000	0.029	24.14	0.005	0.013	1.94×10^{-7}	1–17	0.019	35.97	0.004	0.011	4.67×10^{-6}	1–30
Glycerol	10	0.010	68.02	0.002	0.006	1.53×10^{-9}	1–20	0.017	40.00	0.002	0.006	1.68×10^{-9}	1–30
	30	0.009	77.27	0.002	0.006	3.09×10^{-7}	1–28	0.017	39.63	0.003	0.007	5.90×10^{-9}	1–30
	100	0.016	43.54	0.004	0.011	1.63×10^{-6}	1–20	0.015	46.74	0.004	0.010	1.78×10^{-6}	1–30
	300	0.022	31.97	0.006	0.013	1.40×10^{-7}	1–20	0.016	42.19	0.005	0.013	3.07×10^{-5}	1–30
	1000	0.028	24.48	0.004	0.012	1.32×10^{-6}	1–31	0.018	38.44	0.003	0.008	2.92×10^{-8}	1–30

Doubling time (dt) was calculated following the equation: $dt = \log_e(2)/\mu$. Standard error, 1SE, (SE) and confidence interval (CI) are given for growth rate fitting, and Prob > F refers to the ANOVA test and concludes that at 0.05 level, the fitting function is significantly better than the function $y = $ constant.
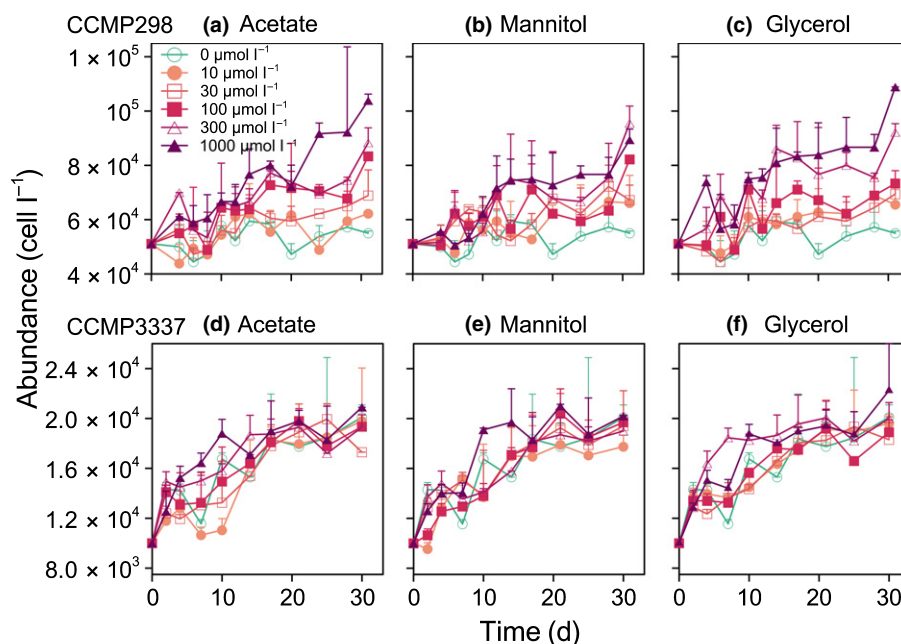

Fig. 2 Cell abundances of CCMP298 *Cruciplacolithus neohelis* (a–c) and CCMP3337 *Chrysotila carterae* (d–f) during the 30-d time course in the dark with the addition of acetate (a, d), mannitol (b, e) or glycerol (c, f) at concentrations of 10 (closed circle), 30 (open square), 100 (closed square), 300 (open triangle) or 1000 (closed triangle) μmol l⁻¹. Open circle symbols on the green line indicate the unamended control. Error bars indicate technical duplicates for cell counts.

treatments, whereas it decreased to an average of 6.7 μm (SD = ± 0.1 μm) in the dark in all treatments (Table 2). As confirmed by one-way ANOVA there was no difference in cell size between the control and augmented treatments in light ($F_{(3,36)}$ = 0.003, $P = 0.999$). The same was confirmed when the treatments were compared in the dark for each compound concentration with the control, for acetate ($F_{(5,54)} = 0.087$, $P = 0.994$), for mannitol ($F_{(5,54)} = 0.086$, $P = 0.994$) and for glycerol ($F_{(5,54)} = 0.034$, $P = 0.999$).

Chrysotila carterae exhibited similar amounts of organic and inorganic carbon content during the 30-d experiments. Both PIC and POC decreased from 20 pg to an average of 15 pg

(a) CCMP298
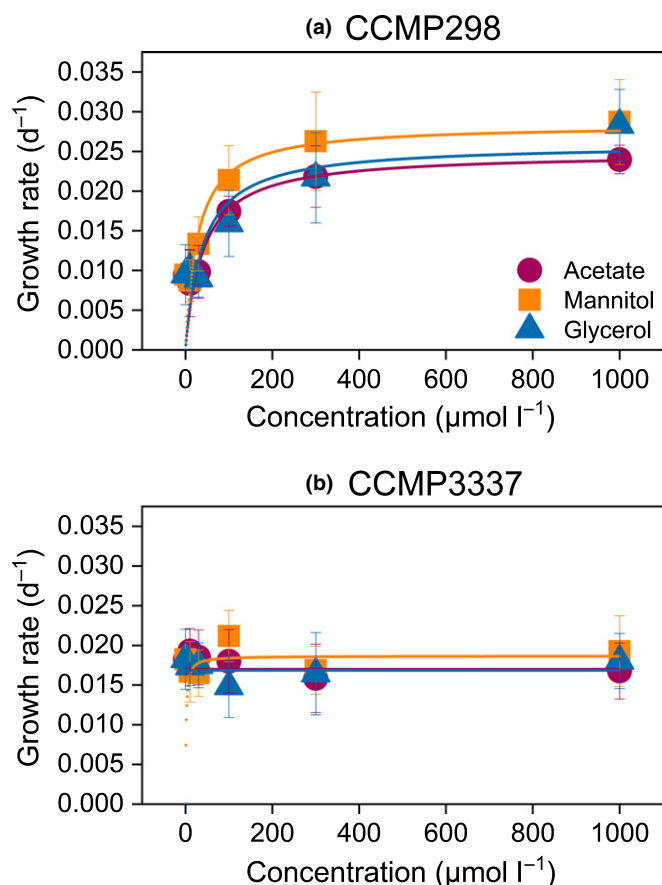
(b) CCMP3337

Fig. 3 Growth rate plotted against the different concentrations of the three organic compounds during the 30-d batch growth experiment for CCMP298 *Cruciplacolithus neohelis* (a) and CCMP3337 *Chrysotila carterae* (b). Curves were fitted according to a nonlinear Michaelis–Menten model, equation: $y = V_{max} \times x/(K_m + x)$. Missing values for *C. carterae* growth were because the curve fit failed. Error bars indicate standard error (1SE) for growth rate. K_m, affinity with which the cells were taking up the organics, aka half-saturation coefficient; V_{max}, maximum rate of growth or uptake.

(SD = ± 2 pg) for all light treatments and to 10 pg (SD = ± 1 pg) when averaged for all dark treatments (Table 2). We also calculated total carbon in each treatment of *C. carterae* by multiplying cell concentrations and cell carbon (Fig. S3). Again, there were no differences when comparing compounds in the light ($F_{(3,36)} = 0.490$, $P = 0.691$) or concentrations in the dark: for acetate ($F_{(5,54)} = 0.941$, $P = 0.462$), for mannitol ($F_{(5,54)} = 0.243$, $P = 0.941$) and for glycerol ($F_{(5,54)} = 1.634$, $P = 0.166$). However, after performing a linear fit for each dark treatment, we found that a significant increase in total carbon occurred between day 2 and day 30 for treatments with concentrations of acetate 30 µmol l^{-1}, mannitol 100 and 300 µmol l^{-1} and glycerol 10 and 30 µmol l^{-1} (Fig. S4).

Uptake kinetics

In the time-course experiments V_{max} values could be considered as a measure of heterotrophic capacity, as it is the upper limit for uptake. Values for V_{max} for uptake at 24 h for *C. neohelis* were 2

$\times 10^{-13}$, 1×10^{-13} and 3×10^{-13} mol cell^{-1} d^{-1} for acetate, mannitol and glycerol, respectively. For *C. carterae*, V_{max} values for uptake were 1×10^{-12}, 1×10^{-13} and 2×10^{-13} mol cell^{-1} d^{-1} for acetate, mannitol and glycerol, respectively (Fig. 4). Plots of uptake velocity vs substrate concentration generally showed increasing saturation behaviour (as opposed to being linear functions) with increasing length of the incubation. For 15 min uptake experiments the kinetics were generally linear. For acetate, the uptake velocities saturated with concentration in as little as 1 h, for mannitol, saturation kinetics were only observed at 24 h while, for glycerol, saturation behaviour was most pronounced at 24 h (Fig. S5). To maximise the signal-to-noise, we chose uptake velocities for 24 h for determination of the Michaelis–Menten model and we were able to calculate the V_{max} and K_m values. Detailed K_m and V_{max} values for uptake are given in Table 3 for the two coccolithophore species.

The K_m values were in the range 1.3×10^{-3} mol l^{-1} (SE = ± 2.3×10^{-4}, *C. neohelis*, glycerol) to 1.8×10^{-6} mol l^{-1} (SE = ± 5.2×10^{-7}, *C. carterae*, mannitol) (Fig. 5). Comparison with the K_m values calculated from the growth experiment was possible for *C. neohelis* and a similar range 10^{-5} mol l^{-1} was noted for acetate and mannitol (Fig. 5). This suggested that the concentration dependence for uptake for acetate and mannitol in *C. neohelis* was similar to the concentration dependence for growth (i.e. they were taking up the carbon compounds and immediately incorporating them into carbon biomass with no luxury consumption).

Fixation of [^{14}C]DOC into the PIC fraction

We recorded net incorporation of [^{14}C]DOC radioactivity into the PIC fraction, with the highest activity in coccoliths observed in the acetate experiments (Fig. 6). The strength of the signal increased with concentration, with a maximum calcification of 1.72×10^{-15} mol cell^{-1} d^{-1} for *C. neohelis* and 5.84×10^{-15} mol cell^{-1} d^{-1} for *C. carterae* at a concentration of 10^{-3} mol l^{-1}. The percentage of incorporation of [^{14}C]acetate into particulate vs organic carbon ranged from 0.43% at a concentration 10^{-7} mol l^{-1} to 1.31% at a concentration of 10^{-4} mol l^{-1} for *C. neohelis*. For *C. carterae*, it ranged from 0.21% at the concentration of 10^{-7} mol l^{-1} to 0.53% at the concentration of 10^{-3} mol l^{-1}. A similar increase with concentration was observed for mannitol and glycerol for *C. neohelis* (Fig. 6). Conclusions for *C. carterae* for these two compounds were not possible. We note that the calculation procedure was to subtract the radioactivity of the formalin-killed control from the radioactivity of each treatment. In a few cases (notably *C. carterae* for mannitol and glycerol) where the formalin-killed number was higher, we assumed zero net incorporation (Fig. 6).

Assimilation of DOC

The pulse–chase experiments showed that virtually all the [^{14}C]-labelled DOC compounds taken up were assimilated into the cells as nonexchangeable pools. At 3 h post chase, cells on average lost only 8% (SD = ± 10.25 Bq) of the radioactivity taken up

Table 2 Mean cell size (MCS) for CCMP3337 *Chrysotila carterae* in light and dark conditions on day 2 and day 30 with corresponding standard deviation of a frequency distribution (SD) calculated from Moxi Z raw data on effective cell diameter.

DOC	Conc. (µmol l^{-1})	Day (2)				Day 30			
		MCS (µm)	SD	POC (pg)	PIC (pg)	MCS (µm)	SD	POC (pg)	PIC (pg)
Light									
Control	0	9.11	2.63	19.72	19.28	7.84	2.10	14.41	14.48
Acetate	100	8.97	2.49	19.09	18.72	8.25	2.03	16.01	15.94
Mannitol	100	8.38	2.45	16.54	16.42	7.96	2.11	14.88	14.91
Glycerol	100	8.41	2.39	16.70	16.56	8.15	2.17	15.60	15.57
Dark									
Control	0	8.04	2.15	15.17	15.17	6.57	1.75	9.93	10.30
Acetate	10	8.12	2.65	15.50	15.48	6.63	1.89	10.12	10.48
	30	8.18	2.37	15.73	15.69	6.76	1.84	10.55	10.88
	100	8.13	2.32	15.55	15.52	6.47	1.71	9.62	10.00
	300	8.04	2.23	15.18	15.18	6.54	1.78	9.84	10.21
	1000	8.03	2.28	15.15	15.15	6.43	1.83	9.51	9.90
Mannitol	10	7.87	2.29	14.53	14.59	6.69	1.74	10.31	10.66
	30	8.18	2.30	15.73	15.69	6.50	1.76	9.71	10.09
	100	8.10	2.27	15.44	15.42	6.83	2.02	10.76	11.09
	300	8.05	2.28	15.23	15.23	6.69	1.71	10.33	10.68
	1000	7.92	2.23	14.72	14.76	6.42	1.73	9.46	9.85
Glycerol	10	8.07	2.29	15.30	15.29	6.93	1.64	11.12	11.42
	30	7.60	2.29	13.48	13.62	6.53	1.69	9.82	10.20
	100	7.98	2.32	14.92	14.95	6.54	1.70	9.83	10.20
	300	7.86	2.26	14.49	14.55	6.65	1.79	10.18	10.54
	1000	7.83	2.11	14.35	14.42	6.54	1.79	9.84	10.21

Organic carbon content (POC) and inorganic carbon content (PIC) were calculated following equations for coccolithophores published by Villiot *et al.* (2021). The experiment used *C. carterae* cells of 9.59 µm (SD ± 3.03 µm) MCS.
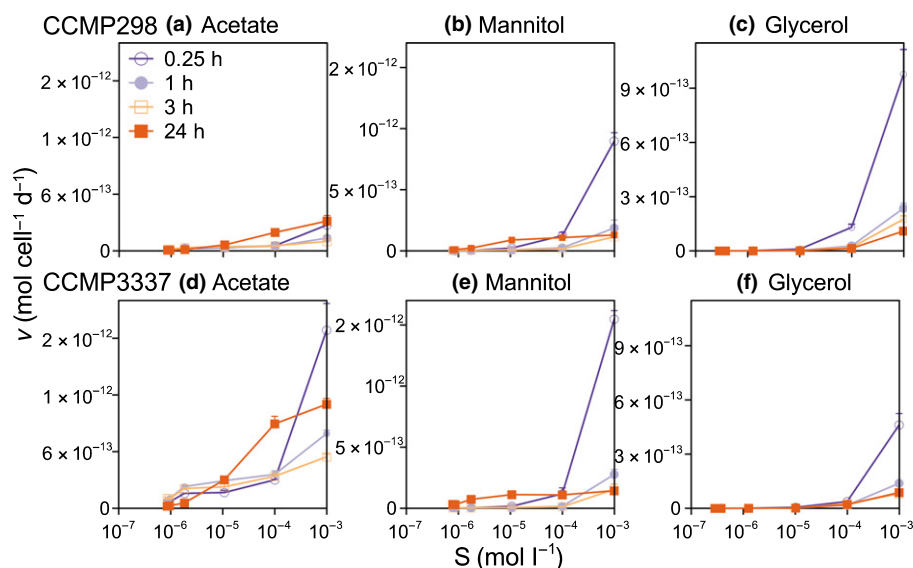
Fig. 4 Uptake velocity of [^{14}C]-labelled organic compounds plotted against substrate concentration (S) at 0.25, 1, 3 and 24 h of the time-course uptake kinetics experiment for [^{14}C]acetate (a, d), [^{14}C]mannitol (b, e), and [^{14}C]glycerol (c, f) for CCMP298 *Cruciplacolithus neohelis* (a–c) and CCMP3337 *Chrysotila carterae* (d–f). Error bars represent SD of triplicate measurements for uptake velocity.

during the time-course experiment (Fig. 7) indicating that organic compounds taken up were not exchangeable after flooding the cells with unlabelled forms. *Cruciplacolithus neohelis* exhibited a transient increase in the radioactivity signal during the pulse–chase experiment with acetate, when at higher concentrations the radioactivity increased up to 10%, 3 h post chase. *Cruciplacolithus neohelis* also experienced a somewhat larger drop

in radioactivity (*c.* 27%) when exposed to mannitol at concentrations in the 10^{-6} to 10^{-5} mol l^{-1} range. *Chrysotila carterae* exhibited the smallest (4%) and most stable (SD = ± 1.31 Bq) loss of radioactivity following the chase with cold glycerol.

Finally, both *C. neohelis* and *C. carterae* took up the greatest amount of acetate per cell, followed by mannitol, and glycerol after a 1-d incubation (Fig. 8). Moreover, the absolute cell

Table 3 Michaelis–Menten kinetics.

DOC	Time (h)	K_m (mol l^{-1})	SE K_m	CI K_m	V_{max} (mol cell^{-1} d^{-1})	SE V_{max}	CI V_{max}	r^2
		Cruciplacolithus neohelis (CCMP298)						
Acetate	0.25	2.63×10^{-6}	9.36×10^{-7}	2.60×10^{-6}	4.99×10^{-14}	1.03×10^{-14}	2.87×10^{-14}	0.841
	1	2.05×10^{-6}	4.63×10^{-7}	1.29×10^{-6}	5.04×10^{-14}	6.79×10^{-15}	1.88×10^{-14}	0.886
	3	1.95×10^{-6}	3.02×10^{-7}	8.37×10^{-7}	5.59×10^{-14}	5.33×10^{-15}	1.48×10^{-14}	0.937
	24	2.49×10^{-5}	3.04×10^{-6}	8.44×10^{-6}	2.21×10^{-13}	2.54×10^{-14}	7.06×10^{-14}	0.992
Mannitol	0.25	6.24×10^{-4}	3.05×10^{-4}	8.46×10^{-4}	1.43×10^{-12}	4.59×10^{-13}	1.27×10^{-12}	0.908
	1	1.64×10^{-3}	7.62×10^{-4}	2.12×10^{-3}	4.97×10^{-13}	1.44×10^{-13}	4.01×10^{-13}	1.000
	3	1.31×10^{-6}	8.34×10^{-7}	2.31×10^{-6}	1.04×10^{-14}	2.69×10^{-15}	7.47×10^{-15}	0.438
	24	1.05×10^{-5}	1.71×10^{-6}	4.74×10^{-6}	1.40×10^{-13}	1.83×10^{-14}	5.09×10^{-14}	0.958
Glycerol	0.25	8.69×10^{-3}	1.75×10^{-2}	3.97×10^{-2}	9.56×10^{-12}	1.74×10^{-11}	3.93×10^{-11}	1.000
	1	2.94×10^{-2}	3.03×10^{-1}	6.85×10^{-1}	7.13×10^{-12}	7.31×10^{-11}	1.65×10^{-10}	0.853
	3	2.94×10^{-3}	5.81×10^{-4}	1.31×10^{-3}	6.97×10^{-13}	1.03×10^{-13}	2.34×10^{-13}	1.000
	24	1.32×10^{-3}	2.34×10^{-4}	5.29×10^{-4}	2.56×10^{-13}	2.61×10^{-14}	5.90×10^{-14}	1.000
		Chrysotila carterae (CCMP3337)						
Acetate	0.25	2.32×10^{-6}	7.03×10^{-7}	1.95×10^{-6}	3.08×10^{-13}	2.33×10^{-14}	6.47×10^{-14}	0.923
	1	4.45×10^{-6}	1.92×10^{-6}	5.32×10^{-6}	5.96×10^{-13}	1.17×10^{-13}	3.26×10^{-13}	0.821
	3	2.88×10^{-6}	7.23×10^{-7}	2.01×10^{-6}	4.29×10^{-13}	7.16×10^{-14}	1.99×10^{-13}	0.870
	24	3.98×10^{-5}	3.21×10^{-6}	8.92×10^{-6}	1.18×10^{-12}	8.56×10^{-14}	2.38×10^{-13}	0.987
Mannitol	0.25	1.32×10^{-3}	8.18×10^{-4}	2.27×10^{-3}	3.60×10^{-12}	1.57×10^{-12}	4.37×10^{-12}	0.931
	1	1.57×10^{-1}	98.6×10^{-1}	2.74×10^{-1}	4.40×10^{-11}	2.75×10^{-9}	7.64×10^{-9}	1.000
	3	3.35×10^{-3}	5.53×10^{-3}	1.54×10^{-2}	6.79×10^{-13}	8.65×10^{-13}	2.40×10^{-12}	0.120
	24	1.76×10^{-6}	5.19×10^{-7}	1.44×10^{-6}	1.24×10^{-13}	1.45×10^{-14}	4.02×10^{-14}	0.896
Glycerol	0.25	4.07×10^{-3}	8.18×10^{-3}	2.27×10^{-2}	2.15×10^{-12}	4.20×10^{-12}	1.17×10^{-11}	0.914
	1	2.00×10^{-3}	7.26×10^{-4}	2.02×10^{-3}	4.17×10^{-13}	1.39×10^{-13}	3.85×10^{-13}	0.979
	3	9.82×10^{-4}	4.45×10^{-4}	1.23×10^{-3}	1.61×10^{-13}	7.18×10^{-14}	1.99×10^{-13}	0.982
	24	6.91×10^{-4}	3.43×10^{-5}	9.52×10^{-5}	1.49×10^{-13}	7.19×10^{-15}	2.00×10^{-14}	0.999

K_m and V_{max} calculated from cellular uptake data using a nonlinear curve fit Michaelis–Menten model, equation: $y = V_{max} * x/(K_m + x)$ for CCMP298 *Cruciplacolithus neohelis* and CCMP3337 *Chrysotila carterae*. K_m (mol l^{-1}) is substrate concentration at which the reaction rate is half of V_{max} (mol cell^{-1} d^{-1}) maximum uptake rate. Calculated standard errors, 1SE, (SE), confidence intervals half-widths (CI) and coefficients of determination (r^2) are given.

content steadily increased during the time course when the strains were exposed to acetate. The cellular uptake in the highest concentration of acetate (10^{-4} mol l^{-1}) reached 3×10^{-13} and 10^{-12} mol cell^{-1} for the *C. neohelis* and *C. carterae,* respectively, after 24 h (Fig. 8). Both strains exhibited a slight drop in the cellular uptake at the 1 h time point when exposed to higher concentrations of mannitol (10^{-5} to 10^{-4} mol l^1). The highest cellular uptake at 24 h for mannitol was *c.* 10^{-13} mol cell^{-1} for both strains (Fig. 8). For glycerol, *C. neohelis* similarly exhibited a drop in the total cellular content at 1 h in the same higher concentration range and reached 10^{-13} mol cell^{-1} maximal quota at highest concentration. The absolute cellular quantity of glycerol steadily increased over 24 h; for *C. neohelis* it reached 9×10^{-14} mol cell^{-1} and for *C. carterae* it reached 8×10^{-14} mol cell^{-1} (Fig. 8).

Discussion

None of the three hypotheses were rejected for *C. neohelis* as it was able to: (1) grow in darkness on organic compounds; (2) take up these compounds actively; and (3) assimilate all organic compounds immediately into mostly nonexchangeable pools. The growth hypothesis was rejected for *C. carterae*, during our 30-d experiments. However, it did take up organic compounds and we found that *C. carterae* assimilated them in relatively nonexchangeable pools. Therefore, our results suggest that osmotrophy

could be an important strategy for survival of these coccolithophore species in darkness, albeit the uptake and growth rates are extremely slow compared with light controls.

Growth in darkness: evolutionary and ecological implications

Cruciplacolithus neohelis and *C. carterae* survived for 30 d in darkness (and divided) using DOC compared with unamended controls. This was in accordance with experiments performed by Blankley (1971), who grew *Emiliania huxleyi* and *C. carterae* on glycerol through 5–20 transfers for 20–49 d in darkness. Based on these results, we can hypothesise that osmotrophy could provide additional nutritional flexibility and support long-term survival of coccolithophores in darkness. This would apply to both the subeuphotic twilight zone as well as the post-Cretaceous asteroid impact period when light intensities were presumed to be well below that required for photosynthesis.

Gibbs *et al.* (2020) showed that mixotrophic phagotrophy was responsible for the recovery of species diversity after the almost complete eradication of coccolithophores during the K/Pg boundary. They supported their claim with morphological analysis of K/Pg survivors and an eco-evolutionary model. However, phagotrophy leaves did not explain the survival of coccolithophores lacking flagellar openings (Hagino *et al.*, 2015), particularly for the extant *C. neohelis*, which has coastal ecology and
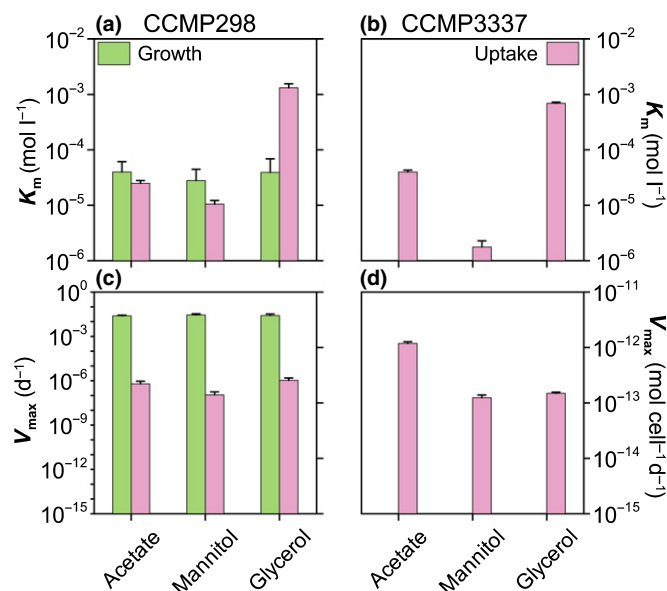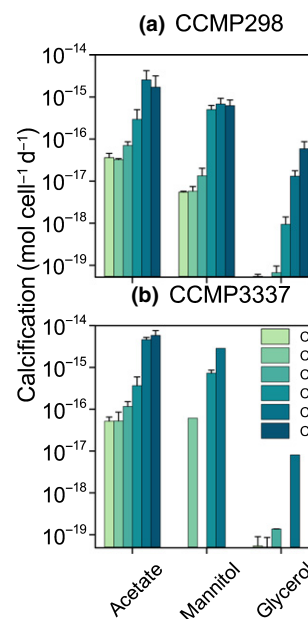
Fig. 5 Comparison of the K_m and V_{max} values calculated for growth and time-course uptake (at 24 h) experiments for (a, c) CCMP298 *Cruciplacolithus neohelis* and (b, d) CCMP3337 *Chrysotila carterae* using a nonlinear curve fit Michaelis–Menten model, equation: $y = V_{max} \times x/(K_m + x)$. (a, b) K_m (mol l^{-1}) is the substrate concentration at which the growth/uptake rate is half of maximum rate at saturation. (c, d) V_{max} indicates calculated maximum values for growth and uptake that are presented on different y-axis and have different units: d^{-1} for growth on the left and mol cell^{-1} d^{-1} for uptake on the right. Error bars indicate SE for the nonlinear curve fit (1SE). K_m, affinity with which the cells were taking up the organics, aka half-saturation coefficient; V_{max}, maximum rate of growth or uptake.

Fig. 6 Radioactivity recorded at 24 h in the inorganic carbon fraction for (a) CCMP298 *Cruciplacolithus neohelis* and (b) CCMP3337 *Chrysotila carterae* from the [^{14}C]-microdiffusion analysis, which separates the particulate organic carbon (POC) fraction from the particulate inorganic carbon (PIC) fraction. C1–C6 represent the concentrations of [^{14}C]-labelled and unlabelled organic compounds added to the kinetics experiment (Supporting Information Table S1) in which C1 is the lowest concentration and C6 is the highest concentrations. Error bars represent the SD of triplicate measurements. Note that the calculation procedure was to subtract the radioactivity of the formalin-killed control from the radioactivity of each treatment; in a few cases in which the formalin-killed number was higher, we assumed zero net incorporation.

produces motile cells (Kawachi & Inouye, 1994). Our results on osmotrophy could support an additional nutritional strategy for survival during the prolonged darkness.

Moreover, certain coccolithophore species (e.g. *Florisphaera profunda*) are regularly found below 200 m (Beaufort *et al.*, 2008) where light intensities do not support net autotrophy. Due to this, they presumably have alternative nutritional strategies to autotrophy, such as mixotrophy (Poulton *et al.*, 2017). As autotrophic biomass is commonly found deeper than 1% light depth (Marra *et al.*, 2014), osmotrophy in the oceans' twilight zone would be a mechanism to expand the niche space of photosynthetically active plankton cells. Acetate concentrations in the ocean are in the micromolar range (King, 1991), while analysis of mannitol and glycerol in saline samples remains problematic to this day. Nevertheless, DOC represents the second largest bioavailable carbon pool in the ocean, after the *c.* 50-fold larger pool of DIC (Hansell & Orellana, 2021). We have shown in our previous work that coccolithophores can indeed metabolise a wide range of organic compounds in the dark (Godrijan *et al.*, 2020). Although the uptake rate for individual organic compounds is slow, the combination of the many organic compounds present in seawater could be the reason why they maintain their growth in the deep euphotic and subeuphotic zones of the ocean. With this work, we further support this hypothesis as we found dark growth in *C. neohelis*.

In dark conditions with low concentrations of organics, growth rates were extremely slow, when compared with growth rates in light. This would be expected, as universal trade-offs between growth and physiological acclimation/survival exist in conditions that induce metabolic transitions (Vasi & Lenski, 1999; Basan *et al.*, 2020). Indeed, one can expect that, for photosynthetic algae, the acclimation to darkness might be slow. However, we suggest that darkness may have triggered the onset of a survival mode, at the cost of cell division. Osmotrophs have evolved cellular adaptations that include high-affinity transporters that facilitate rapid uptake (Glibert & Legrand, 2006).

Smaller cells have more transporters per volume of cell, assuming a constant number of transporters per unit area of membrane. This could effectively increase the velocity of uptake. The more prominent decreases in cell size in darkness in our experiments could have had the same effect. In general, diversified nutritional strategies, such as mixotrophy, require more investment of energy and are likely to be responsible for lower growth rates if compared with nutritional specialists (Rothhaupt, 1996). Analysis of the carbon content of *C. carterae* during the 30-d growth experiments, in which there was no significant growth, indicated that the decrease in carbon content was probably at the expense of the internal cellular carbon pool. It is likely that the stored carbon would partition within 1 d, shortly after the onset of darkness.
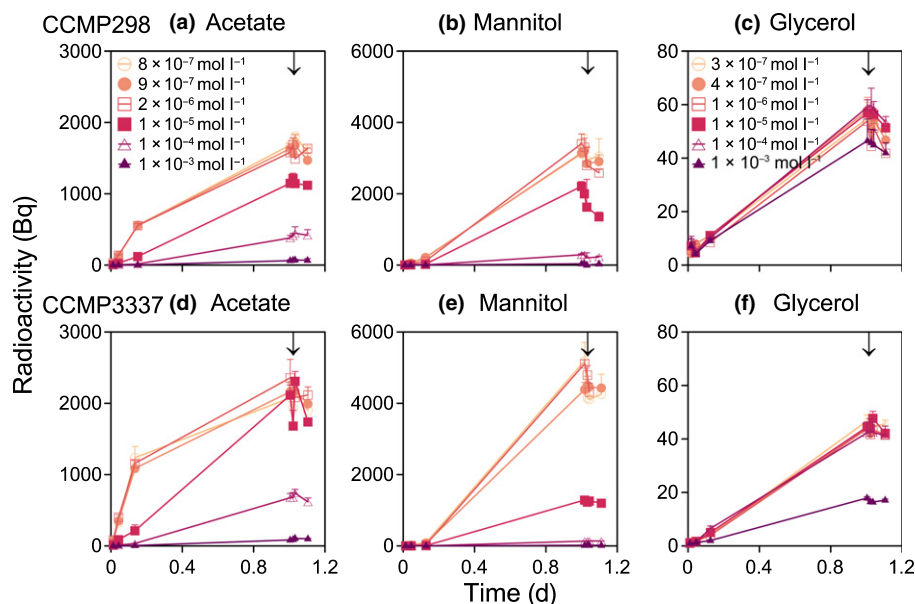
Fig. 7 Measured radioactivity [Bq] over time during the time-course uptake experiments and pulse–chase experiments (after 1 d and marked with arrows) for [^{14}C]acetate (a, d), [^{14}C]mannitol (b, e), and [^{14}C]glycerol (c, f) for CCMP298 *Cruciplacolithus neohelis* (a–c) and CCMP3337 *Chrysotila carterae* (d–f). Initial concentrations of [^{14}C]-labelled and unlabelled organic compounds added to the kinetics experiments are given in the legends (see also Supporting Information Table S1). Error bars represent the SD of triplicate measurements.
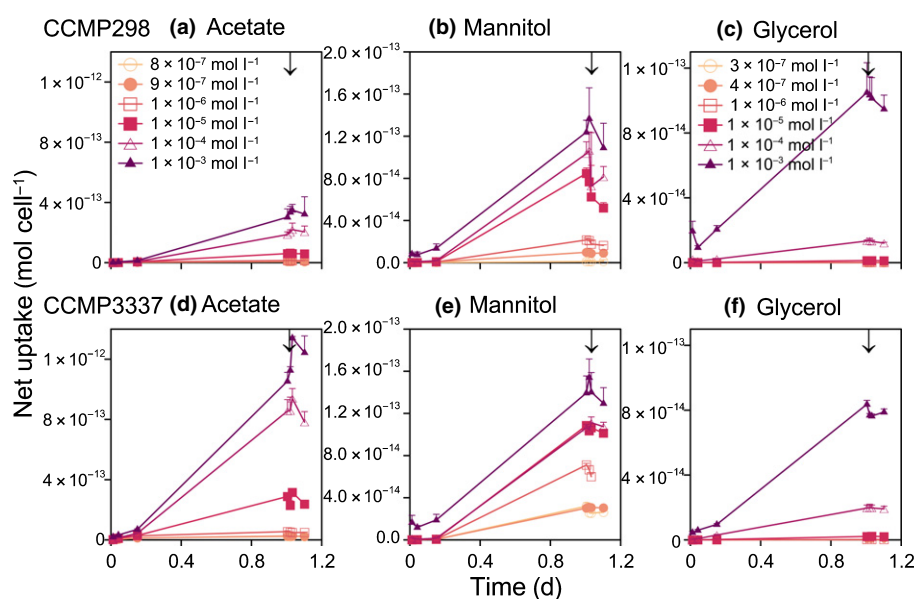
Fig. 8 Net cellular uptake of the [^{14}C]acetate (a, d), [^{14}C]mannitol (b, e), and [^{14}C]glycerol (c, f) during the time-course uptake experiments and pulse–chase experiments for CCMP298 *Cruciplacolithus neohelis* (a–c) and CCMP3337 *Chrysotila carterae* (d–f). Error bars represent the SD of triplicate measurements. Measured radioactivity after 1 d is marked with an arrow.

Thereafter, cells were probably unable to fix enough carbon because cellular uptake was so low. However, analysis of individual dark treatments without time zero showed a slight increase in total POC in several of them (Fig. S4), suggesting the possibility that cells would take up enough carbon over a longer period to cause further division.

Uptake and assimilation

Uptake of acetate by microalgae has been well investigated. Acetate is taken up via a transporter-mediated mechanism (Droop, 1974; Gimenez *et al.*, 2003) and can be used for heterotrophic growth in darkness (Neilson & Lewin, 1974). But, if sodium acetate is used as a substrate, the pH rises and could be

toxic for many microorganisms at high concentrations (Ratledge *et al.*, 2001). Nevertheless, it seems that as long as the level of acetate remains low, microalgae can use it as its sole carbon source (Perez-Garcia *et al.*, 2011). Zotina *et al.* (2003) reported that cyanobacteria *Planktothrix rubescens* efficiently took up acetate even under low-light conditions, demonstrating a preference for DOC uptake as a carbon source rather than photosynthesis in these photic conditions. In experiments with natural plankton populations at low substrate concentrations (10^{-7} mol l^{-1}), Wright & Hobbie (1966) reported uptake values for acetate in the range 10^{-5} mg l^{-1} h^{-1}, whereas our results for *C. neohelis* were between 10^{-7} and 10^{-3} mg l^{-1} h^{-1} (acetate concentrations of 10^{-7}–10^{-4} mol l^{-1}). Therefore, our results suggest that *C. neohelis* can actively take up acetate and grow successfully

in the dark. However, the 30-d dark growth experiment was too short to confirm the growth of *C. carterae*.

Conversely, few studies have been done on the uptake of mannitol in microalgae (Lewis & Smith, 1967; Yee, 2015). It is still unclear how it enters the algal cells, but mannitol membrane transporters are found in bacteria, plants and fungi (Roossien & Robillard, 1984; Patel & Williamson, 2016). Colman *et al.* (1986) studied the uptake of mannitol by four species of *Chlorella* and found that the uptake was species dependent, but cells of *C. vulgaris* were found impermeable to mannitol. However, Yee (2015) did report on mannitol having a stimulating effect on the growth of the green alga, *Monoraphidium griffithii*. Our study revealed that the two coccolithophore species were able to take up mannitol in darkness and both species showed saturation kinetics when measured over 24 h (Fig. 4b,e), suggestive of a membrane transporter for mannitol.

Glycerol can be used as a substrate by many algae, both in the light and in darkness (Perez-Garcia *et al.*, 2011; Penhaul Smith *et al.*, 2020), and successful heterotrophic growth of coccolithophores was demonstrated in high concentrations of glycerol by Blankley (1971). We found here that *C. neohelis* was able to grow in low glycerol concentrations (Fig. 2c) with indications of saturation kinetics (Fig. 4c). Glycerol was found to freely pass through biological membranes (Wright *et al.*, 1969) and enter the cell by simple Fickian diffusion (Neilson & Lewin, 1974). However, there are other reports on different transport mechanisms for glycerol. Tsay *et al.* (1971) found that transport of glycerol by the bacteria, *Pseudomonas aeruginosa*, involves a binding protein responsible for recognition of glycerol. Additionally, studies with *Dunaliella parva* (Hard & Gilmour, 1996) showed that the uptake of glycerol is active, they confirmed the energy dependence of the glycerol transport system by its response to external salinity. These inconsistent results suggest that further investigations of glycerol transport in microalgae are warranted.

For successful utilisation of organic carbon compounds for growth, osmotrophs need both a transport system to get compounds into the cell against a concentration gradient and the presence of enzymatic pathways to convert compounds into suitable precursors for carbon metabolism (Azma *et al.*, 2011). Our results suggest active uptake of organic compounds over 24 h incubations, for acetate for both coccolithophore species (Fig. 8), but the fate of each compound within the cell is unclear. Nonetheless, our results of the pulse–chase experiments confirmed that all organic compounds were assimilated by these coccolithophore species into mostly nonexchangeable pools.

We showed that the affinity, or the concentration dependence, of *C. neohelis* for cellular uptake was generally similar to the concentration dependence for growth for the tested compounds (compare the K_m values in Fig. 5). This suggests the balanced assimilation of organic compounds into biomass (Shuter, 1979). Muñoz-Marín *et al.* (2020) reviewed the uptake rates of different organics for *Prochlorococcus* and *Synechococcus* and showed that they were in the range 10^{-18} mol cell^{-1} d^{-1}. These rates were well below the cellular uptake rates that we recorded for these larger coccolithophores (Fig. 4).

A possible link between the alkalinity pump and the biological carbon pump?

One unexpected result from these experiments was the appearance of [^{14}C] activity (which was taken up as [^{14}C]DOC compounds by coccolithophores) into coccolithophore PIC. The percentage of incorporation of [^{14}C]DOC into PIC was as high as 1.3% per cell. This is the first such observation of this phenomenon. One unlikely explanation for this is that the radiolabelled organic carbon molecules were somehow directly incorporated into PIC via an unknown biochemical pathway. Alternatively, the more likely explanation is that the carbon in the DOC may have been rapidly assimilated by the coccolithophores, respired as [^{14}C]DIC and subsequently incorporated into coccolith calcite through standard calcification reactions (Brownlee *et al.*, 2021). The results presented here do not allow us to discern the mechanism of how the carbon was incorporated into PIC.

It has traditionally been assumed that coccolithophore calcification derives the PIC from DIC (namely bicarbonate), not DOC. If [^{14}C]DOC were being metabolised by the coccolithophores and respired as CO_2, then indeed this is yet more evidence of DOC osmotrophy and assimilation by coccolithophores. But the implications go further. Indeed, the entire paradigm of the alkalinity pump assumes that coccolithophores are assimilating bicarbonate alkalinity in the surface ocean into dense coccoliths that ultimately sink to the depth at which they dissolve, releasing ('pumping') the bicarbonate alkalinity at depth.

An osmotrophic lifestyle of coccolithophore – in which calcification is incorporating carbon originating from DOC, which sinks to the depth where it dissolves and releases bicarbonate at depth – raises fundamental questions about the role of the alkalinity pump and how it controls the alkalinity balance in the sea. If coccolith carbon does not originate from bicarbonate but instead from DOC carbon, then the alkalinity pump paradigm needs to be revised. This is because coccolithophore calcification would not necessarily be at the expense of DIC. Instead, a fraction of the sinking calcite carbon could be associated with the largest organic carbon pool in the sea, the DOC pool. Uptake of DOC and transport to depth has typically been associated with the biological carbon pump (Rost & Riebesell, 2004). Therefore, potential rapid incorporation of DOC carbon into coccoliths inextricably merges the alkalinity and biological carbon pumps in a way not before appreciated.

Author contributions

JG, DTD and WMB all contributed to the design of the research. JG and DTD performed the research. JG and WMB did the data analysis and interpretation. JG prepared the manuscript with contributions from DTD and WMB.

ORCID

William M. Balch (iD) https://orcid.org/0000-0003-4926-195X
David T. Drapeau (iD) https://orcid.org/0000-0002-5822-8433
Jelena Godrijan (iD) https://orcid.org/0000-0003-2586-0034

Data availability

The data that support the findings of this study are available from the corresponding author upon request. They are also available from the Biological and Chemical Oceanography Data Management Office (BCO-DMO; https://www.bco-dmo.org/).

References

Adl SM, Bass D, Lane CE, Lukeš J, Schoch CL, Smirnov A, Agatha S, Berney C, Brown MW, Burki F *et al.* 2019. Revisions to the classification, nomenclature, and diversity of eukaryotes. *Journal of Eukaryotic Microbiology* 66: 4–119.

Avrahami Y, Frada MJ. 2020. Detection of phagotrophy in the marine phytoplankton group of the coccolithophores (Calcihaptophycidae, Haptophyta) during nutrient-replete and phosphate-limited growth. *Journal of Phycology* 56: 1103–1108.

Azma M, Mohamed MS, Mohamad R, Rahim RA, Ariff AB. 2011. Improvement of medium composition for heterotrophic cultivation of green microalgae, *Tetraselmis suecica*, using response surface methodology. *Biochemical Engineering Journal* 53: 187–195.

Bach LT, Mackinder LCM, Schulz KG, Wheeler G, Schroeder DC, Brownlee C, Riebesell U. 2013. Dissecting the impact of CO_2 and pH on the mechanisms of photosynthesis and calcification in the coccolithophore *Emiliania huxleyi*. *New Phytologist* 199: 121–134.

Balch WM. 1986. Exploring the mechanism of ammonium uptake in phytoplankton with an ammonium analogue, methylamine. *Marine Biology* 92: 163–171.

Balch WM, Bowler BC, Drapeau DT, Lubelczyk LC, Lyczkowski E, Mitchell C, Wyeth A. 2019. Coccolithophore distributions of the North and South Atlantic Ocean. *Deep Sea Research Part I: Oceanographic Research Papers* 151: 103066.

Balch WM, Drapeau DT, Fritz JJ. 2000. Monsoonal forcing of calcification in the Arabian Sea. *Deep Sea Research Part II: Topical Studies in Oceanography* 47: 1301–1337.

Basan M, Honda T, Christodoulou D, Hörl M, Chang Y-F, Leoncini E, Mukherjee A, Okano H, Taylor BR, Silverman JM *et al.* 2020. A universal trade-off between growth and lag in fluctuating environments. *Nature* 584: 470–474.

Beaufort L, Couapel M, Buchet N, Claustre H, Goyet C. 2008. Calcite production by coccolithophores in the south east Pacific Ocean. *Biogeosciences* 5: 1101–1117.

Blankley WF. 1971. *Auxotrophic and heterotrophic growth and calcification in coccolithophorids*. Ph.D., University of California, San Diego La Jolla, CA.

Bown PR. 1998. *Calcareous nannofossil biostratigraphy*. London, UK: Chapman & Hall (Kluwer Academic).

Bown PR, Lees JA, Young JR. 2004. Calcareous nannoplankton evolution and diversity through time. In: Thierstein HR, Young JR, eds. *Coccolithophores: from molecular processes to global impact*. Berlin/Heidelberg, Germany: Springer, 481–508.

Brownlee C, Langer G, Wheeler GL. 2021. Coccolithophore calcification: changing paradigms in changing oceans. *Acta Biomaterialia* 120: 4–11.

Brownlee C, Taylor AR. 2004. Calcification in coccolithophores: a cellular perspective. In: Thierstein HR, Young JR, eds. *Coccolithophores: from molecular processes to global impact*. Berlin/Heidelberg, Germany: Springer, 31–49.

Colman B, Brickell PC, Gehl KA. 1986. The uptake of mannitol and sorbitol by a species of *Chlorella* (Chlorophyceae). *Journal of Phycology* 22: 436–440.

Droop MR. 1974. Heterotrophy of carbon. In: Stewart WDP, ed. *Algal physiology and biochemistry*. Berkeley, CA, USA: University of California Press, 530–559.

Flynn KJ, Mitra A, Anestis K, Anschütz AA, Calbet A, Ferreira GD, Gypens N, Hansen PJ, John U, Martin JL *et al.* 2019. Mixotrophic protists and a new paradigm for marine ecology: where does plankton research go now? *Journal of Plankton Research* 41: 375–391.

Gibbs SJ, Bown PR, Ward BA, Alvarez SA, Kim H, Archontikis OA, Sauterey B, Poulton AJ, Wilson J, Ridgwell A. 2020. Algal plankton turn to hunting to survive and recover from end-Cretaceous impact darkness. *Science Advances* 6: eabc9123.

Gimenez R, Nuñez MF, Badia J, Aguilar J, Baldoma L. 2003. The gene yjcG, cotranscribed with the gene acs, encodes an acetate permease in *Escherichia coli*. *Journal of Bacteriology* 185: 6448–6455.

Glibert PM, Legrand C. 2006. The diverse nutrient strategies of harmful algae: focus on osmotrophy. In: Granéli E, Turner JT, eds. *Ecology of harmful algae*. Berlin/Heidelberg, Germany: Springer, 163–175.

Godrijan J, Drapeau D, Balch WM. 2020. Mixotrophic uptake of organic compounds by coccolithophores. *Limnology and Oceanography* 65: 1410–1421.

Godrijan J, Young JR, Marić Pfannkuchen D, Precali R, Pfannkuchen M. 2018. Coastal zones as important habitats of coccolithophores: a study of species diversity, succession, and life-cycle phases. *Limnology and Oceanography* 63: 1692–1710.

Guillard RRL, Hargraves PE. 1993. *Stichochrysis immobilis* is a diatom, not a chrysophyte. *Phycologia* 32: 234–236.

Hagino K, Young JR, Bown PR, Godrijan J, Kulhanek DK, Kogame K, Horiguchi T. 2015. Re-discovery of a 'living fossil' coccolithophore from the coastal waters of Japan and Croatia. *Marine Micropaleontology* 116: 28–37.

Haldane JBS. 1957. Graphical methods in enzyme chemistry. *Nature* 179: 832.

Hallegraeff GM, Anderson DM, Cembella AD, Enevoldsen HO. 2003. *Manual on harmful marine microalgae*. Paris, France: UNESCO.

Hansell DA, Orellana MV. 2021. Dissolved organic matter in the global ocean: a primer. *Gels* 7: 128.

Hard BC, Gilmour DJ. 1996. The uptake of organic compounds by *Dunaliella parva* CCAP 19/9. *European Journal of Phycology* 31: 217–224.

Houdan A, Probert I, Zatylny C, Véron B, Billard C. 2006. Ecology of oceanic coccolithophores. I. Nutritional preferences of the two stages in the life cycle of *Coccolithus braarudii* and *Calcidiscus leptoporus*. *Aquatic Microbial Ecology* 44: 291–301.

Jeon Y-C, Cho C-W, Yun Y-S. 2006. Combined effects of light intensity and acetate concentration on the growth of unicellular microalga *Haematococcus pluvialis*. *Enzyme and Microbial Technology* 39: 490–495.

Jones H, Scrobola Z, Bralower T. 2021. Size and shape variation in the calcareous nannoplankton genus *Braarudosphaera* following the Cretaceous/Paleogene (K/Pg) mass extinction: clues as to its evolutionary success. *Paleobiology*. doi: 10.1017/pab.2021.15.

Kawachi M, Inouye I. 1994. Observations on the flagellar apparatus of a coccolithophorid, *Cruciplacolithus neohelis* (Prymnesiophyceae). *Journal of Plant Research* 107: 53–62.

Keller MD, Selvin RC, Claus W, Guillard RRL. 1987. Media for the culture of oceanic ultraphytoplankton. *Journal of Phycology* 23: 633–638.

King GM. 1991. Measurement of acetate concentrations in marine pore waters by using an enzymatic approach. *Applied and Environmental Microbiology* 57: 3476–3481.

Langer G, Taylor AR, Walker CE, Meyer EM, Ben Joseph O, Gal A, Harper GM, Probert I, Brownlee C, Wheeler GL. 2021. Role of silicon in the development of complex crystal shapes in coccolithophores. *New Phytologist* 231: 1845–1857.

Lewis DH, Smith DC. 1967. Sugar alcohols (polyols) in fungi and green plants. *New Phytologist* 66: 143–184.

Marra JF, Lance VP, Vaillancourt RD, Hargreaves BR. 2014. Resolving the ocean's euphotic zone. *Deep Sea Research Part I: Oceanographic Research Papers* 83: 45–50.

Muñoz-Marín MC, Gómez-Baena G, López-Lozano A, Moreno-Cabezuelo JA, Díez J, García-Fernández JM. 2020. Mixotrophy in marine picocyanobacteria: use of organic compounds by *Prochlorococcus* and *Synechococcus. ISME Journal* 14: 1065–1073.

Neilson AH, Lewin RA. 1974. The uptake and utilization of organic carbon by algae: an essay in comparative biochemistry. *Phycologia* 13: 227–264.

Nelson PH. 2002. A permeation theory for single-file ion channels: corresponding occupancy states produce Michaelis-Menten behavior. *Journal of Chemical Physics* 117: 11396–11403.

O'Grady J, Morgan JA. 2011. Heterotrophic growth and lipid production of *Chlorella protothecoides* on glycerol. *Bioprocess and Biosystems Engineering* 34: 121–125.

Paasche E. 2001. A review of the coccolithophorid *Emiliania huxleyi* (Prymnesiophyceae), with particular reference to growth, coccolith formation, and calcification-photosynthesis interactions. *Phycologia* 40: 503–529.

Paasche E, Brubak S. 1994. Enhanced calcification in the coccolithophorid *Emiliania huxleyi* (Haptophyceae) under phosphorus limitation. *Phycologia* 33: 324–330.

Parke M, Adams I. 1960. The motile *Crystallolithus hyalinus* (Gaarder & Markali) and non-motile phases in the life history of *Coccolithus pelagicus* (Wallich) Schiller. *Journal of the Marine Biological Association of the United Kingdom* 39: 263–274.

Parke M, Manton I, Clarke B. 1956. Studies on marine flagellates: III. Three further species of *Chrysochromulina. Journal of the Marine Biological Association of the United Kingdom* 35: 387–414.

Parsons TR, Maita Y, Lalli CM. 1984. *A manual of chemical and biological methods for seawater analysis.* Toronto, ON, Canada: Pergamon Press.

Patel TK, Williamson JD. 2016. Mannitol in plants, fungi, and plant-fungal interactions. *Trends in Plant Science* 21: 486–497.

Penhaul Smith JK, Hughes AD, McEvoy L, Day JG. 2020. Tailoring of the biochemical profiles of microalgae by employing mixotrophic cultivation. *Bioresource Technology Reports* 9: 100321.

Perez-Garcia O, Escalante FME, de-Bashan LE, Bashan Y. 2011. Heterotrophic cultures of microalgae: metabolism and potential products. *Water Research* 45: 11–36.

Poulton AJ, Holligan PM, Charalampopoulou A, Adey TR. 2017. Coccolithophore ecology in the tropical and subtropical Atlantic Ocean: new perspectives from the Atlantic meridional transect (AMT) programme. *Progress in Oceanography* 158: 150–170.

Qiao H, Wang G. 2009. Effect of carbon source on growth and lipid accumulation in *Chlorella sorokiniana* GXNN01. *Chinese Journal of Oceanology and Limnology* 27: 762.

Ratledge C, Kanagachandran K, Anderson AJ, Grantham DJ, Stephenson JC. 2001. Production of docosahexaenoic acid by *Crypthecodinium cohnii* grown in a pH-auxostat culture with acetic acid as principal carbon source. *Lipids* 36: 1241–1246.

Reuss L, Altenberg GA. 2013. Chapter 2 – mechanisms of ion transport across cell membranes. In: Alpern RJ, Moe OW, Caplan M, eds. *Seldin and Giebisch's the kidney, 5th edn.* Oxford, UK: Academic Press, 45–66.

Ribeiro S, Berge T, Lundholm N, Andersen TJ, Abrantes F, Ellegaard M. 2011. Phytoplankton growth after a century of dormancy illuminates past resilience to catastrophic darkness. *Nature Communications* 2: 311.

Roossien FF, Robillard GT. 1984. Mannitol-specific carrier protein from the *Escherichia coli* phosphoenolpyruvate-dependent phosphotransferase system can be extracted as a dimer from the membrane. *Biochemistry* 23: 5682–5685.

Rost B, Riebesell U. 2004. Coccolithophores and the biological pump: responses to environmental changes. In: Thierstein HR, Young JR, eds. *Coccolithophores: from molecular processes to global impact.* Berlin, Heidelberg: Springer, 99–125.

Rothhaupt KO. 1996. Utilization of substitutable carbon and phosphorus sources by the mixotrophic chrysophyte *Ochromonas* sp. *Ecology* 77: 706–715.

Shuter B. 1979. A model of physiological adaptation in unicellular algae. *Journal of Theoretical Biology* 78: 519–552.

Silva HR, Prete CEC, Zambrano F, de Mello VH, Tischer CA, Andrade DS. 2016. Combining glucose and sodium acetate improves the growth of *Neochloris oleoabundans* under mixotrophic conditions. *AMB Express* 6: 10.

Taylor AR, Brownlee C. 2016. Calcification. In: Borowitzka MA, Beardall J, Raven JA, eds. *The physiology of microalgae.* Cham, Switzerland: Springer International Publishing, 301–318.

Tsay SS, Brown KK, Gaudy ET. 1971. Transport of glycerol by *Pseudomonas aeruginosa. Journal of Bacteriology* 108: 82–88.

Vajda V, Ocampo A, Ferrow E, Koch CB. 2015. Nano particles as the primary cause for long-term sunlight suppression at high southern latitudes following the Chicxulub impact — evidence from ejecta deposits in Belize and Mexico. *Gondwana Research* 27: 1079–1088.

Vasi FK, Lenski RE. 1999. Ecological strategies and fitness tradeoffs in *Escherichia coli* mutants adapted to prolonged starvation. *Journal of Genetics* 78: 43–49.

Villiot N, Poulton AJ, Butcher ET, Daniels LR, Coggins A. 2021. Allometry of carbon and nitrogen content and growth rate in a diverse range of coccolithophores. *Journal of Plankton Research* 43: 511–526.

de Vries J, Monteiro F, Wheeler G, Poulton A, Godrijan J, Cerino F, Malinverno E, Langer G, Brownlee C. 2021. Haplo-diplontic life cycle expands coccolithophore niche. *Biogeosciences* 18: 1161–1184.

Winter A, Siesser WG. 1994. *Coccolithophores.* Cambridge, UK: Cambridge University Press.

Wood BJB, Grimson PHK, German JB, Turner M. 1999. Photoheterotrophy in the production of phytoplankton organisms. In: Osinga R, Tramper J, Burgess JG, Wijffels RH, eds. *Progress in industrial microbiology.* Amsterdam, the Netherlands: Elsevier, 175–183.

Worden AZ, Follows MJ, Giovannoni SJ, Wilken S, Zimmerman AE, Keeling PJ. 2015. Rethinking the marine carbon cycle: factoring in the multifarious lifestyles of microbes. *Science* 347: 1257594.

Wright EM, Diamond JM, Smyth DH. 1969. Patterns of non-electrolyte permeability. *Proceedings of the Royal Society of London. Series B: Biological Sciences* 172: 227–271.

Wright RR, Hobbie JE. 1966. Use of glucose and acetate by bacteria and algae in aquatic ecosystems. *Ecology* 47: 447–464.

Wu H, Green M, Scranton MI. 1997. Acetate cycling in the water column and surface sediment of Long Island Sound following a bloom. *Limnology and Oceanography* 42: 705–713.

Yee W. 2015. Feasibility of various carbon sources and plant materials in enhancing the growth and biomass productivity of the freshwater microalgae *Monoraphidium griffithii* NS16. *Bioresource Technology* 196: 1–8.

Zhuang G-C, Peña-Montenegro TD, Montgomery A, Montoya JP, Joye SB. 2019. Significance of acetate as a microbial carbon and energy source in the water column of Gulf of Mexico: implications for marine carbon cycling. *Global Biogeochemical Cycles* 33: 223–235.

Zotina T, Köster O, Jüttner F. 2003. Photoheterotrophy and light-dependent uptake of organic and organic nitrogenous compounds by *Planktothrix rubescens* under low irradiance. *Freshwater Biology* 48: 1859–1872.

Supporting Information

Additional Supporting Information may be found online in the Supporting Information section at the end of the article.

Fig. S1 Experimental schemes.

Fig. S2 Results of Tukey's pairwise test.

Fig. S3 Total carbon in all treatments of *Chrysotila carterae.*

Fig. S4 Linear fit on total carbon dark treatments of *Chrysotila carterae*.

Fig. S5 Michaelis–Menten fits plotted for dark uptake.

Table S1 Final concentrations of organic compounds used in experiments.

Table S2 Statistical parameters of nonlinear curve fit Michaelis–Menten model for growth rate vs concentration plot.

Please note: Wiley Blackwell are not responsible for the content or functionality of any Supporting Information supplied by the authors. Any queries (other than missing material) should be directed to the *New Phytologist* Central Office.